European Journal of Neuroscience, Vol. 26, pp. 1407–1420, 2007 doi:10.1111/j.1460-9568.2007.05774.x

Genetic ablation of NMDA receptor subunit NR3B in mouse reveals motoneuronal and nonmotoneuronal phenotypes

Stephan Niemann,[1,2,3,*,§] Hiroaki Kanki,[4,†,§] Yasuyuki Fukui,[5] Keizo Takao,[5,6] Masahiro Fukaya,[7] Meri N. Hynynen,[2] Michael J. Churchill,[1,‡] Jeremy M. Shefner,[8] Roderick T. Bronson,[9] Robert H. Brown, Jr.,[2,3] Masahiko Watanabe,[7] Tsuyoshi Miyakawa,[5,6] Shigeyoshi Itohara[4] and Yasunori Hayashi[1]

[1]RIKEN-MIT Neuroscience Research Center, The Picower Institute for Learning and Memory, Department of Brain and Cognitive Sciences, Massachusetts Institute of Technology, 77 Massachusetts Avenue, Cambridge, MA 02139, USA
[2]Cecil B. Day Laboratory for Neuromuscular Research
[3]Department of Neurology, Harvard Medical School, MassGeneral Institute for Neurodegenerative Disease, Massachusetts General Hospital, Charlestown, MA 02129, USA
[4]Laboratory for Behavioral Genetics, RIKEN Brain Science Institute, Wako, Saitama 351-0198, Japan
[5]Genetic Engineering and Functional Genomics Unit, Horizontal Medical Research Organization, Kyoto University Graduate School of Medicine, Kyoto 606-8501, Japan
[6]Division of Systems Medical Science, Institute for Comprehensive Medical Science, Fujita Health University, Toyoake, Aichi 470-1192, Japan
[7]Department of Anatomy, Hokkaido University School of Medicine, Sapporo 060-8638, Japan
[8]Department of Neurology, Upstate Medical University, 750 East Adams Street, Syracuse, New York 13210, USA
[9]Department of Pathology, Harvard Medical School, Boston, MA 02115, USA

Keywords: excitatory synaptic transmission, gene targeting, motor neuron, mouse behaviour, NMDA type glutamate receptor subunit NR3B

Abstract

NR3B is a modulatory subunit of the NMDA receptor, abundantly expressed in both cranial and spinal somatic motoneurons and at lower levels in other regions of the brain as well. Recently, we found the human NR3B gene (*GRIN3B*) to be highly genetically heterogeneous, and that ~10% of the normal European-American population lacks NR3B due to homozygous occurrence of a null allele in the gene. Therefore, it is especially important to understand the phenotypic consequences of the genetic loss of NR3B in both humans and animal models. We here provide results of behavioral analysis of mice genetically lacking NR3B, which is an ideal animal model due to homogeneity in genetic and environmental background. The NR3B$^{-/-}$ mice are viable and fertile. Consistent with the expression of NR3B in somatic motoneurons, the NR3B$^{-/-}$ mice showed a moderate but significant impairment in motor learning or coordination, and decreased activity in their home cages. Remarkably, the NR3B$^{-/-}$ mice showed a highly increased social interaction with their familiar cage mates in their home cage but moderately increased anxiety-like behaviour and decreased social interaction in a novel environment, consistent with the inhibitory role of NR3B on the functions of NMDA receptors. This work is the first reporting of the functional significance of NR3B *in vivo* and may give insight into the contribution of genetic variability of NR3B in the phenotypic heterogeneity among human population.

Introduction

The *N*-methyl-D-aspartate receptor (NMDAR) is a heterotetramer composed of the functionally essential NR1 subunit and of NR2 and NR3 subunits, which add functional diversity (Seeburg, 1993; Nakanishi & Masu, 1994). The NR3 subclass is an inhibitory subunit which, when assembled with NR1 and NR2, reduces the Ca^{2+} permeability as well as the overall current (Ciabarra *et al*., 1995; Sucher *et al*., 1995; Nishi *et al*., 2001). It has also been reported that, when NR3 is combined only with NR1, it forms an excitatory glycinergic channel (Chatterton *et al*., 2002).

NR3B was the second member of the NR3 class of subunits to be discovered (Andersson *et al*., 2001; Nishi *et al*., 2001; Chatterton *et al*., 2002; Matsuda *et al*., 2002). In adult animals, it is mainly expressed in somatic motoneurons but also at lower levels in other regions including the hippocampus and cerebellum (Nishi *et al*., 2001; Chatterton *et al*., 2002; Matsuda *et al*., 2002; Bendel *et al*., 2005; Fukaya *et al*., 2005; GENSAT database). During development, NR3B is detected in the anterior olfactory nucleus, piriform cortex, subicular cortex, hippocampus, amygdala and cerebellum (GENSAT database) but again the amount seems to be limited. However, despite these

Correspondence: Dr Stephan Niemann, at *Current address below.
E-mail: niste@mit.edu *or* niemann.stephan@gmail.com
or: Yasunori Hayashi, as above.
E-mail: yhayashi@mit.edu

**Current address*: Epigenomics AG, Kleine Präsidentenstraße 1, 10178 Berlin, Federal Republic of Germany.

†*Current address*: Department of Physiology, Keio University School of Medicine, 35 Shinanomachi, Shinjuku-ku, Tokyo 160-8582, Japan

‡*Current address*: Department of Psychology, University of Michigan, 530 Church Street, Ann Arbor, MI 48109-1043, USA

§S.N. and H.K. contributed equally to this paper.

Received 1 May 2007, revised 10 July 2007, accepted 19 July 2007

functions and expression patterns, the role of NR3B *in vivo* has been obscure due to a lack of specific pharmacological reagents that would allow an isolation of its function.

Previously we explored the possibility that genetic dysfunction of the NR3B gene might be involved in the pathogenesis of motor neuron disease. As a consequence, we found that the human NR3B gene is highly genetically polymorphic (Niemann *et al*., in press). Of note, we observed that ~ 10% of the European–American population are homozygous for a 4-bp insertion in exon 3, which truncates the protein and creates a functionally null mutant lacking all membrane-associated domains. The frequent observation of the 4-bp insertion in normal individuals indicates that it represents a polymorphism. The NR3B-null allele occurs world-wide at allele frequencies between 0 and 0.38 and appears to have arisen early and once in human evolution, making it especially intriguing to know its functional consequence. We then hypothesized that the loss of NR3B, although not pathogenic, may cause phenotypic variation among human populations and may have a modifying affect on neurological or neuropsychiatric disorders. However, humans are not ideal for detecting subtle phenotypic changes due to significant diversity in genetic and environmental background between individuals.

We therefore generated a mouse model genetically lacking NR3B to test whether the loss of NR3B results in any phenotype in a controlled background. The $NR3B^{-/-}$ mice showed a moderate but significant impairment in motor coordination and/or learning, possibly resulting from a lack of NR3B in motoneurons. The animals also had altered emotional levels which cannot be easily explained by motoneuronal expression but could be due to a low level of expression in other neurons. Our study is the first to reveal *in vivo* functions of NR3B. The common loss of NR3B in humans may contribute to an as-yet-undiscerned variation in human behaviour as well.

Materials and methods

The animal experiments were approved by the RIKEN Institutional Animal Care and Use Committee, the Institutional Reviewer Committees of Kyoto University Graduate School of Medicine and Hokkaido University School of Medicine, the Animal Care Committee at the Massachusetts General Hospital, Harvard Medical School, and the Committee for Animal Care, Massachusetts Institute of Technology.

Construction of targeting vector

Using an EST clone (accession number AW045848) containing a part of exon 3 of mouse NR3B as a probe, a mouse genomic library of the 129/SV strain (BACPAC Resources Center) was screened to obtain the entire gene. The exon–intron structure was determined by comparing the cDNA sequence of NR3B (accession number AF396649; Nishi *et al*., 2001) with the mouse genomic sequence. To construct the targeting vector, the ~ 3.9-kb Xba I/Hinc II fragment located immediately upstream of the NR3B gene and the ~ 5.6-kb BamH I/Sac II fragment covering the region from intron 1 (partially) to exon 9 of NR3B were subcloned at up- and downstream of a PGK-neo expression cassette (Rudnicki *et al*., 1992) flanked by a loxP sequence pair. The combined fragment was inserted upstream of the diphtheria toxin A-fragment (DT-A) in an expression vector (Yagi *et al*., 1993). In the resultant targeting vector, the exon 1 containing the initiation codon of NR3B was replaced with the neo cassette, while the rest of the genomic structure remained intact (Fig. 1A). The targeting vector was linearized at the Sph I site located downstream of the DT-A before electroporation.

Generation of mutant mice (Gomi et al.,*1995)*

Embryonic stem (ES) cells derived from 129 J mouse strain (embryonic day 14 cells) were electroporated with 20 μg of linearized targeting vector DNA and selected for G418 resistance (175 μg/mL). Correct homologous recombination was verified by Southern blot analysis after Hind III digestion using ~ 510 bp 5′ or ~ 520 bp 3′ external probe (Fig. 1B). Recombinants were obtained at a frequency of 12 per ~ 800 G418-resistant clones. Five targeted ES clones were independently injected into C57BL/6J blastocysts, and two of them yielded chimeric mice capable of transmitting the targeted NR3B allele through the germ line. To excise the PGK-neo cassette, germline-transmitted chimeras were first mated with Cre females, which expresses Cre in their zygotes (Sakai & Miyazaki, 1997). The correct excision of the PGK-neo cassette was confirmed by PCR with a primer pair flanking the PGK-neo cassette. The mice carrying the mutated NR3B allele were backcrossed to C57BL/6J for at least eight generations before analyses. Genotypes were determined by Southern hybridization or PCR analysis of tail genomic DNAs. PCR was performed at 94 °C for 30 s, 57 °C for 45 s and 72 °C for 1 min with 30 cycles, with primers to detect knockout alleles (5′-CAA GAC CCA CAG GAG AGA AG-3′ and 5′-CAT CTA GGA GTC ATG CTC CAG-3′) and to detect wild-type (WT) alleles (5′-GTG GTG GCC TCT ATA ACC TT-3′ and 5′-GTC TGG TCT ACA CAG TGA GA-3′).

Histology, immunostaining, RT-PCR and in situ *hybridization*

For histology and immunostaining, the animals were killed by an overdose of pentobarbital (100 mg/kg). The histology of the amygdala was examined with Cresyl violet Nissl staining using coronal microslicer sections (50 μm in thickness). Immunostaining for the NR1-C2 cassette was performed using pepsin-treated paraffin sections through the L3–L5 spinal cord according to a previously published method (Watanabe *et al*., 1998).

For RT-PCR, the animals were anesthetized with CO_2. RNA isolated from the spinal cords of adult $NR3B^{-/-}$ animals and littermates was reverse-transcribed in cDNA using SuperScript II (Invitrogen, Carlsbad, CA, USA). PCR was carried out essentially as described (Nishi *et al*., 2001). As a positive control for RT-PCR, we used a primer pair for GAPDH (sense 5′-TGG AAT CGA GAC AAC ATT GC-3′; antisense 5′-CTG TAG TGG CAG GCT TTT CC-3′).

In situ hybridization was performed in coronal sections of brainstem obtained from $NR3B^{-/-}$ and $^{+/+}$ mice at postnatal day (P)21 using ^{33}P-labelled antisense oligonucleotide probes as described previously (Fukaya *et al*., 2005). The animals were killed with an overdose of pentobarbital (100 mg/kg). For NR3B, a mixture of oligoNR3b-1, oligoNR3b-3 and oligoNR3b-4 located in exon 3 was used. For vesicular acetylcholine transporter (VAchT), an antisense oligonucleotide corresponding to mouse mRNA sequence 2171–2220 was used (accession AF019045). Sections were exposed to nuclear track emulsion (NTB-2; Kodak, Rochester, NY, USA) for 4 weeks. Emulsion-dipped sections were counterstained with methyl green pyronine.

Whole-body pathological examination and ventral root counting

Whole-body pathological examinations were carried out in the Rodent Histopathology Core at The Dana-Farber/Harvard Cancer Center. Mice at 13 months of age were anaesthetized with CO_2, then transcardially perfused, first with 0.9% saline and then with 4% paraformaldehyde. Complete necropsies of animals were performed,

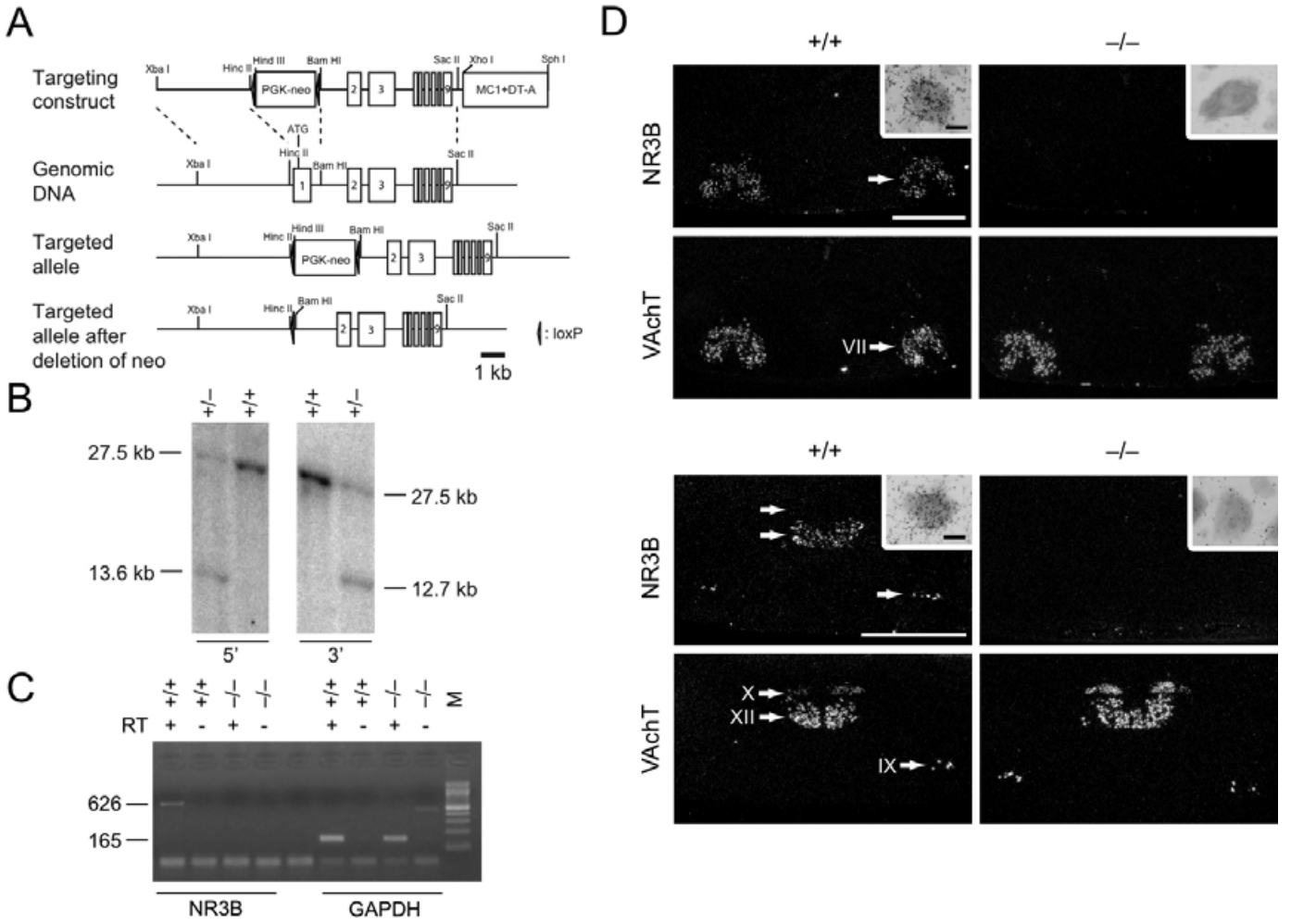

FIG. 1. Targeted disruption of the NR3B gene in mouse. (A) The NR3B gene consists of nine exons in the mouse. The targeting vector was designed to disrupt exon 1 containing the initiator methionine, signal peptide sequence and N-terminal portion of the extracellular protein domain. PGK-neo was later removed by crossing the resultant mouse with a Cre-expressing deleter line. (B) Southern blotting of genomic DNA from ES cells underwent successful recombination ($^{+/-}$) and from parental embryonic day 14 cells, a 129-derived ES cell line, used in this study ($^{+/+}$) with 5′ (left) and 3′ (right) external probes. (C) Confirmation of loss of NR3B mRNA by RT-PCR using RNA from spinal cord of adult NR3B$^{+/+}$ and $^{-/-}$ animals as template. A primer set spanning the junction between exons 2 and 3 (5′ primer) to exon 3 (3′ primer) was used. Samples without reverse transcriptase (RT–) served as negative control and the reactions with GAPDH as positive control. The faint band in the last lane (GAPDH, RT–, NR3B$^{-/-}$) is due to the amplification of genomic DNA carried over from RNA preparation. (D) *In situ* hybridization of NR3B in coronal sections of brain stem from NR3B$^{-/-}$ and $^{+/+}$ animals. A mixture of three oligonucleotide probes against exon 3 was used. Sections contained facial (top, VII), ambiguus (bottom, IX), and hypoglossal (bottom, XII) nuclei. The NR3B signal was detected only in somatic motoneurons of NR3B$^{+/+}$ but not $^{-/-}$ animals. The hybridization using the VAchT probe served as a positive control and appears similar in $^{-/-}$ and $^{+/+}$ animals. Visceral motoneurons in the dorsal motor nucleus of the vagus nerve (bottom, X), were also detected with the VAchT probe but not with NR3B probe. Pictures shown are dark-field images. Inset, higher magnification of motoneurons in bright-field images. Scale bars, 100 μm for dark-field images, 10 μm for insets.

and 6-μm paraffin sections of each organ were prepared, stained with haematoxylin and eosin and examined.

For a detailed morphological analysis, ventral roots of the spinal cord at the lumbar 3 level were dissected immediately following intracardial perfusion and postfixed in 2.5% glutaraldehyde at 4 °C overnight. Roots were osmicated with 1% osmium tetroxide and embedded in an Araldite resin. Sections were cut at 300 nm and stained with toluidine blue. For axon distribution calculations, cross-sections of ventral roots in three mice per genotype were analysed. Images covering the entire root were acquired at 100× magnification, and the axon diameters were measured using the Bioquant software (Bioquant Image Analysis Corporation, Nashville, TN, USA). Axons of all three animals per genotype were lumped together and grouped by diameter into 1-μm bins. The statistical significance of the axon diameter distribution was calculated using one-way ANOVA.

Motor unit number estimation (MUNE)

NR3B$^{-/-}$ mice and their WT littermates (12 months old, female) were anaesthetized by isoflurane inhalation. MUNE was performed using a modification of the incremental technique, as described previously (Shefner *et al*., 2006). The sciatic nerve was stimulated in the proximal thigh using Teflon-insulated 0.7-mm sensory needles (Medtronic, Minneapolis, MN, USA). Motor responses were recorded from a pregelled, self-adhesive surface recording strip (Nicolet, Madison, WI, USA) placed circumferentially around the animal's distal hindlimb. The reference electrode was a monopolar needle placed subcutaneously in the foot, distal to the recording electrode. Stimuli were 0.1-ms pulses delivered through a constant-current stimulator with fine intensity control (Keypoint; Medtronic). Stimulus intensity was increased until compound muscle action potential was maximized. Its amplitude (peak–peak) and latency (to negative onset) were then recorded.

After proper electrode localization, stimulus intensity was slowly increased from subthreshold levels until a small all-or-none response was evoked. The response was established by observing an identical response three or four times. The stimulation intensity was slowly increased until the response increased in a quantal fashion. The increased response was again observed for stability before the trace was accepted for analysis. This process was repeated for a total of 10 increments. Prior to obtaining the incremental responses, a supramaximal response was obtained. This response was used to calculate distal motor latency as well as maximal compound muscle action potential amplitude. Individual motor unit amplitudes were obtained by subtracting the amplitude of each response from that of the prior response. The individual values were averaged to yield an estimate of average single motor unit potential size. This value was divided into the peak–peak amplitude of the maximum compound muscle action potential to yield the MUNE. Data from both right and left legs were pooled for statistical analysis using unpaired *t*-tests.

Behaviour analysis

A behavioral test battery was conducted as described previously (Crawley, 1999; Miyakawa *et al*., 2001, 2003; Takao & Miyakawa, 2006). NR3B$^{-/-}$ mice and their WT littermates ($n = 18$ and 15, unless otherwise specified) were generated by mating heterozygous NR3B$^{+/-}$ mice. The resulting animals were subjected to the behavioral test battery summarized in Table 1. All tests except behaviour monitoring in the home cage were performed between 08.00 and 18.00 h using adult male mice that were at least 9 weeks of age. The animals were housed one per cage in a room with a 12-h light–dark cycle (lights on at 07.00 h) with access to food and water *ad libitum*. After each test, the apparatus was cleaned with diluted sodium hypochlorite solution to prevent a bias due to olfactory cues.

TABLE 1. Behavioral test battery used in this study

Name of test	Results presented in:	Age performed (weeks)
General health	Text	9–11
Neurological screen	Text	9–11
Body weight	Fig. 4	See Fig.
Body temperature	Supplementary Fig. S1	9–11
Wire hang	Supplementary Fig. S1	9–11
Grip strength test	Supplementary Fig. S1	9–11
Light–dark transition	Supplementary Fig. S3	10–11
Open field	Fig. 9	10–11
Elevated plus-maze	Fig. 8	10–12
Hot plate	Supplementary Fig. S2	10–12
Social interaction (novel environment)	Fig. 8	11–12
Rotarod	Fig. 5	11–13
Beam test	Supplementary Fig. S1	11–13
Prepulse inhibition and startle response	Supplementary Fig. S2	12–14
Porsolt forced swim	Supplementary Fig. S3	12–14
24 h Home cage monitoring	Fig. 6	15–17
Food intake	Fig. 4	17–20
Water intake	Fig. 4	17–20
Eight-arm radial maze	Fig. 7	21–23[†] 24–26[‡]

The tests are listed in the order in which they were performed. The ages of the animals at the time of tests are shown in right column. The range indicates the range of the age of animals. [†]Training started; [‡]training ended.

Rotarod (Miyakawa et al., *2003)*

The rotarod test was carried out on a commercially available apparatus (Ugo Basile Accelerating Rotarod, Varese, Italy). The cylinder was 3 cm in diameter with a surface of scored plastic. Mice were confined to a section of the cylinder 6.0 cm long by black Plexiglas dividers. Each mouse was placed on the cylinder, which increased its rotation speed from 4 to 40 r.p.m. over a 5-min period. The latency at which mice either fell off the rotarod or clung to the rod while it turned one full rotation was recorded. Mice that did not fall or cling during the 300-s trial period were removed and given a score of 300.

Activity monitoring and social interaction test in home cage (Miyakawa et al., *2003)*

A system that automatically analyses behaviour in home cages was used to monitor locomotion activity and social behaviour between two mice in a familiar environment. The system consisted of a home cage ($29 \times 18 \times 12$ cm) and a filtered cage top, separated by a 13-cm-high metal stand containing an infrared video camera, which was attached to the top of the stand. Two genetically identical mice that had been housed separately were placed together in a home cage and their behaviour was video-monitored over $\sim$5.5 days. Outputs from the cameras were fed into a Macintosh computer. Images from each cage were captured at a rate of one frame per second. Their locomotor activity was measured by quantifying the number of pixels changed between successive frames. Social interaction was measured by counting the number of particles in each frame: two particles indicated that the mice were not in contact with each other and one particle indicated contact between the two mice.

Elevated plus-maze (Miyakawa et al., *2001)*

The maze consisted of two open (25×5 cm) and two enclosed arms of the same size, with walls 15 cm high. The arms were constructed of black acrylic radiating from a central platform (5×5 cm) to form a plus sign. The entire apparatus was elevated to a height of 55 cm above floor level. Each mouse was placed in the central platform facing one of the open arms. The number of entries into the open and closed arms and the time spent on the open and closed arms were recorded during a 5-min test period.

Social interaction test in a novel environment

Two mice of identical genotypes, that were previously housed in different cages, were placed into a box together ($40 \times 40 \times 30$ cm) and allowed to explore freely for 10 min. Social behaviour was monitored by a CCD camera which was connected to a Macintosh computer. Analysis was performed automatically from images captured at one frame per second. Total duration of contact, number of contacts, number of active contacts, mean duration per contact and total distance traveled were measured. The number of active contacts was defined as follows: distance traveled between two successive frames was calculated for each mouse. If the two mice contacted each other and the distance traveled by either mouse was longer than 5 cm, the behaviour was considered ‘active contact’.

Eight-arm radial maze test (Miyakawa et al., *2001; Takao & Miyakawa, 2006)*

The floor of the maze was made of white Plexiglas, and the wall (25 cm high) consisted of transparent Plexiglas. Each arm

(9 × 40 cm) radiated from an octagonal central starting platform (perimeter 12 × 8 cm) like the spokes of a wheel. Identical food wells (1.4 cm deep and 1.4 cm in diameter) with pellet sensors were placed at the distal end of each arm. The pellet sensors were able to automatically record pellet intake by the mice. The maze was elevated 75 cm above the floor and placed in a dimly lit room with several extra-maze cues. During the experiment, the maze was maintained in a constant orientation. Prior to pretraining, animals were deprived of food until their body weight was reduced to 80–85% of the initial level. In the pretraining session, mice were placed in the maze with their cagemates and allowed to explore and to consume food pellets scattered on the whole maze for a 30-min period. After the initial pretraining, each mouse received another pretraining to take a pellet from each food well after being placed at the distal end of each arm. After this pretraining, acquisition trials were performed. All eight arms were baited with food pellets. Mice were placed on the central platform and allowed to get all eight pellets. A trial was terminated immediately after all eight pellets were consumed or 15 min had elapsed. An 'arm visit' was defined as traveling for > 5 cm from the central platform. The mice were confined in the centre platform for 5 s after each arm choice. For each trial, the number of different arms chosen within the first eight choices, and the number of revisitings, were automatically recorded.

Contextual and cued fear conditioning

Each mouse was placed in a test chamber (26 × 34 × 29 cm) inside a sound-attenuated chamber (O'Hara & Co., Tokyo, Japan) and allowed to explore freely for 2 min. A 60-dB white noise, which served as the conditioned stimulus (CS), was presented for 30 s, followed by a mild (2 s, 0.5 mA) footshock, which served as the unconditioned stimulus (US). Two more CS–US pairings were presented with 2-min interstimulus intervals. To examine shock sensitivity, we measured distance traveled when the foot shock was delivered (from 2 s before the shock to 2 s after the shock, total 6 s). Context testing was conducted 1 day after conditioning in the same chamber. Cued testing with altered context was conducted 1 day after conditioning using a triangular box (35 × 35 × 40 cm) made of white opaque Plexiglas, which was located in a different room. Data acquisition, control of stimuli (i.e. tones and shocks) and data analysis were performed automatically. Images were captured at 1 frame per second. For each pair of successive frames, the size of the of area (pixels) by which the mouse moved was measured. When this area was below a certain threshold (i.e. 20 pixels), the behaviour was judged to be 'freezing'. When the area equalled or exceeded the threshold, the behaviour was considered 'non-freezing'. The threshold (amount of pixels) for determining freezing was determined by adjusting it to the amount of freezing measured by human observation. 'Freezing' that lasted < 2 s was not included in the analysis.

Open-field test (Miyakawa et al.*, 2003)*

To assess spontaneous locomotor activity, mice were placed into the centre of an open-field apparatus (40 × 40 × 30 cm; Accuscan Instruments, Columbus, OH, USA). The chamber was illuminated (100 lux). Motor activity parameters (distance traveled, number of vertical and stereotypic movements, and centre time) were then monitored and recorded over a 120-min period.

Image analysis and statistics

The applications used for the behavioral studies were Image LD, Image EP, Image RM, Image FZ, Image SI and Image HA, written by T.M. based on the public domain NIH Image program (developed at the U.S. National Institutes of Health and available on the Internet at http://rsb.info.nih.gov/nih-image/) and ImageJ program (http://rsb.info.nih.gov/ij/), which were modified for each test by T.M. (available through O'Hara & Co.). Statistical analysis was conducted by using Excel (Microsoft, Redmond, WA, USA), Igor Pro (Wavemetrics, Portland, OR, USA), STATVIEW (SAS institute, Cray, NC, USA) or PRISM (GraphPad, San Diego, CA, USA). Data were analysed using two-tailed *t*-tests, one-way ANOVA, two-way ANOVA or repeated-measures ANOVA and are presented as mean ± SEM.

Web resources

Mouse Gene Expression Nervous System Atlas (GENSAT; Gong *et al*., 2003; Magdaleno *et al*., 2006): http://www.ncbi.nlm.nih.gov/projects/gensat/

Journal of Visualized Experiments (Light–dark Transition Test): http://www.jove.com/Details.htm?id=104&VID = 116

Results

NR3B$^{-/-}$ mice were apparently healthy with a slightly low body weight

We eliminated exon 1, which contains the initiation methionine and subsequent signal peptide, from the NR3B gene (Fig. 1A). We confirmed the loss of expression of NR3B in the spinal cord of adult NR3B$^{-/-}$ animals by using RT-PCR with a primer set spanning the junction between exons 2 and 3 (5′ primer) to exon 3 (3′ primer; Fig. 1C). As expected, a PCR product was not observed with RNA derived from NR3B$^{-/-}$ animals. Consistently, the *in situ* hybridization using oligonucleotide probes against the exon 3 did not show any signal in motoneurons although a VAchT signal was evident at a level similar to that in littermate $^{+/+}$ animals (Fig. 1D). These results showed that the elimination of the exon 1 of the NR3B gene resulted in the loss of expression of, at least, NR3B exons 1–3. Exons 1–3 encode the ligand binding and channel pore regions of NR3B. Even if any protein were expressed from the rest of the exons (exon 4 and downstream), it would be highly unlikely to be functional.

Upon gross inspection, NR3B$^{-/-}$ mice had normal fur, whiskers and posture, and were indistinguishable from $^{+/+}$ mice. Casual trials of righting reflex, whisker touch reflex and ear twitch reflex were also normal. They had similar body temperature (Supplementary material, Appendix. S1, Fig. S1, A) and normal lifespan, and were fertile.

We checked the viability of motoneurons because the loss of NR3B may increase NMDAR activity to abnormal levels, potentially causing excitotoxic damages to motoneurons. Upon tissue inspection, however, spinal motoneurons at different levels appeared normal in number without any sign of cell death such as chromatin condensation or change in the size of the cell body (Fig. 2A). Currently, no good antibody is available to detect NR3B. We therefore carried out immunostaining using NR1 antibody as it forms a complex with NR3B (Watanabe *et al*., 1998; Matsuda *et al*., 2003). Punctate signals were similarly distributed around MAP2-positive somatodendritic regions and also inside perikarya of motoneurons between NR3B$^{-/-}$ and $^{+/+}$ animals (Fig. 2B). This result indicates that loss of NR3B does not largely change the distribution of NR1.

Axon caliber of ventral roots is a sensitive measure of motoneuronal damage (Garcia *et al*., 2003). They were similar in NR3B$^{-/-}$ and $^{+/+}$ animals (Fig. 3A–C). To determine whether there was remodelling of

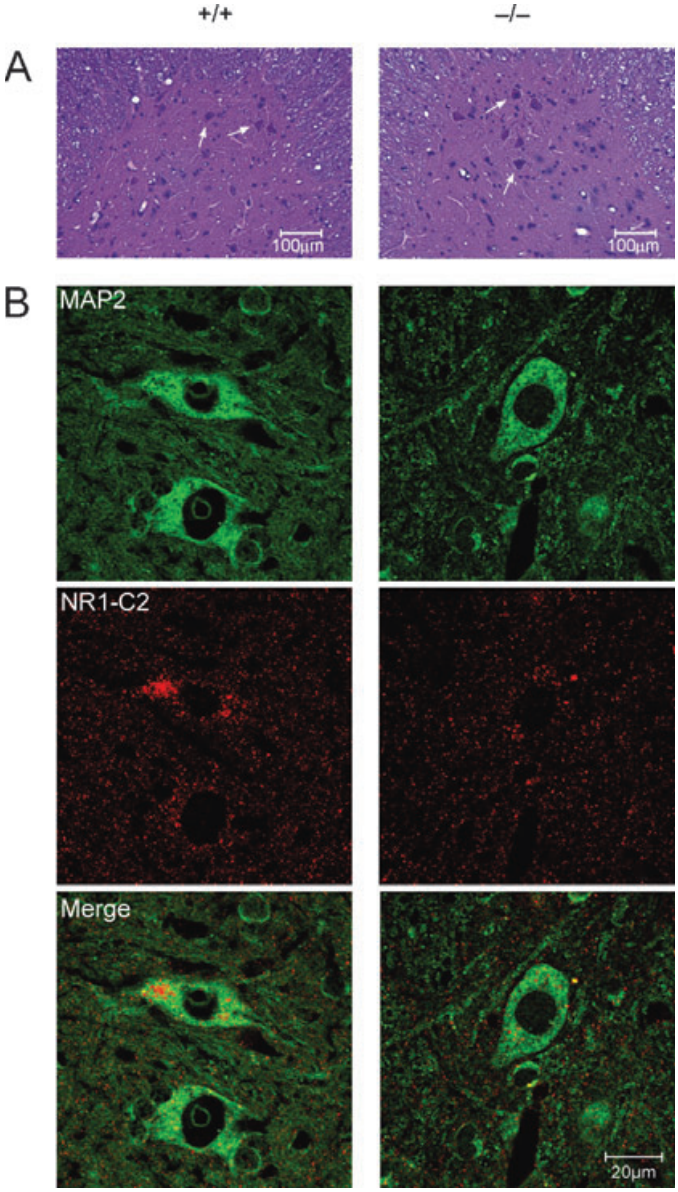

FIG. 2. Motor neurons were preserved in NR3B$^{-/-}$ mice. (A) Ventral horn of spinal cord at the lumbar level from NR3B$^{+/+}$ and $^{-/-}$ animals stained with haematoxylin–eosin. Arrows indicate motoneurons. (B) Immunostaining of NR1-C2 (red) and MAP2 (green) in the section of spinal cord at lumber level 3–5 (L3–5). The staining patterns were largely unchanged between NR3B$^{+/+}$ and $^{-/-}$ animals.

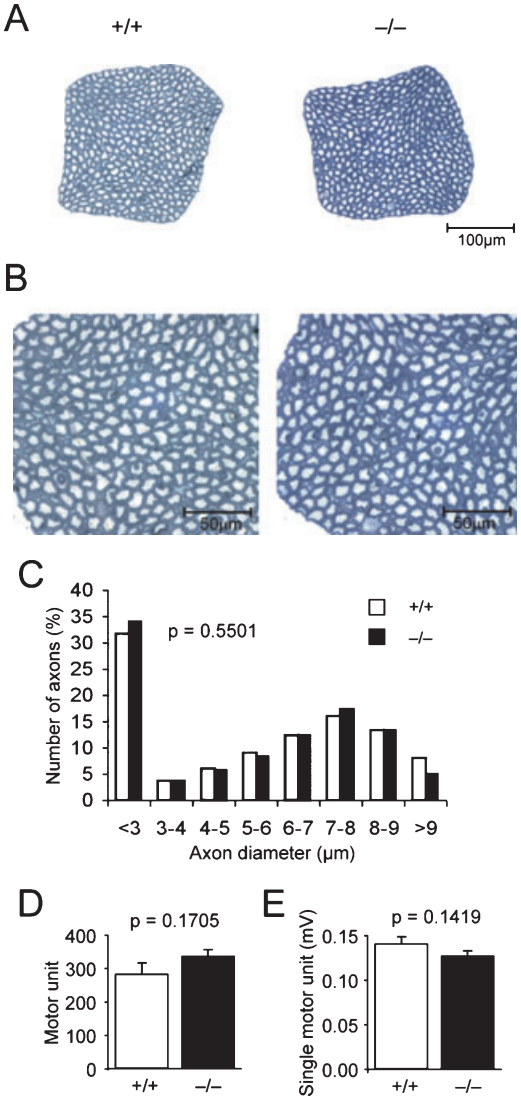

FIG. 3. Axons from motoneurons were morphologically and functionally normal in the NR3B$^{-/-}$ mouse. (A and B) Cross-section of ventral roots at lumbar level 3 (L3) from NR3B$^{+/+}$ and $^{-/-}$ animals. (C) Quantification of diameter of axons. There was no statistically significant difference in the distribution of fiber diameters. Axons with a diameter <3 µm are those from neurons other than α-motoneurons, probably γ-motoneurons, and were not included in the statistical test. Statistical significance was tested using one-way ANOVA. The data were obtained from three each $^{-/-}$ and $^{+/+}$ male animals at 15 months of age. Total numbers of axons were 2488 for $^{-/-}$ and 2231 for $^{+/+}$ animals. Numbers of axons >3 µm were 1711 for $^{-/-}$ and 1460 for $^{+/+}$ animals. (D and E) Estimation of (D) motor unit numbers and (E) single motor unit potential; $n = 16$ for $^{-/-}$ and 6 for $^{+/+}$ animals. Measurements from the two legs were averaged and treated as single data points. Statistical significance was tested using the *t*-test.

the motor unit architecture, we conducted MUNE and measured single motor unit potential by measuring the response of distal hindlimb muscles evoked by sciatic nerve stimulation (Fig. 3D and E). The MUNE reflects the number of motor units innervating a muscle and will decrease in response to axon damage with a concomitant increase in single motor unit potential (Shefner *et al.*, 2006). These two parameters were similar in NR3B$^{-/-}$ and $^{+/+}$ animals. Furthermore, a whole-body pathological examination did not reveal any findings (not shown). Taken together, the NR3B$^{-/-}$ animals did not exhibit any pathological changes overall, which is consistent with the fact that human null-mutants of NR3B do not show any pathological effect (Niemann *et al.*, in press).

Upon further investigation, we found that NR3B$^{-/-}$ animals had a lower body weight, by $\sim$10% (Fig. 4A; $t_{31} = 3.694$, $P = 0.0008$, 16–18 weeks; $t_{31} = 3.95$, $P = 0.0004$, 17–19 week). This was not evident in early adulthood and became evident after 16–18 postnatal weeks and was observed until 13 months, the last time point examined (genotype effect, $F_{1,23} = 9.035$, $P = 0.0063$; genotype × age interaction, $F_{4,92} = 5.112$, $P = 0.0009$). In order to determine whether this change was caused by reduced intake of food or water, we measured these parameters (Fig. 4B and C). There was no significant difference in food intake and only a marginal reduction in water intake (Fig. 4C; genotype effect, $F_{1,17} = 2.367$, $P = 0.1423$ for food intake; genotype effect, $F_{1,17} = 5.061$, $P = 0.0380$ for water

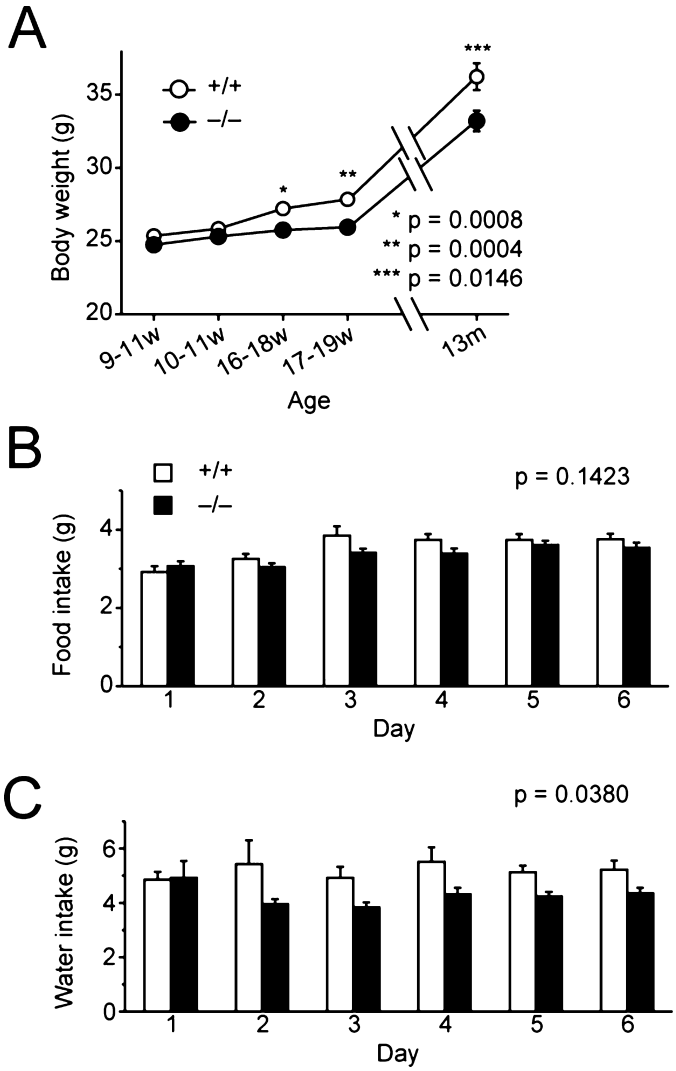

FIG. 4. Reduced weight of NR3B$^{-/-}$ animals. (A) Averaged weight of NR3B$^{-/-}$ and $^{+/+}$ mice was plotted vs. age. w, week; m, month; $n = 18$ for $^{-/-}$, 15 for $^{+/+}$ (9–11 and 17–19 w) or 14 for $^{-/-}$, 11 for $^{+/+}$ (13 m). Statistical significance between genotypes was tested with two-way repeated-measures ANOVA. One-way ANOVA was used to test the statistical significance at each age. (B) Food and (C) water consumption per animal. The animals were caged individually for measurement. Note that intake is not normalized to body weight in this figure. Statistical significance was tested with two-way repeated-measures ANOVA; $n = 10$ for $^{-/-}$ and 9 for $^{+/+}$ animals.

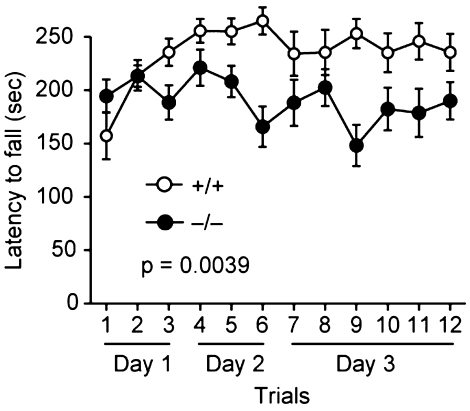

FIG. 5. Impaired performance of NR3B$^{-/-}$ animals in the rotarod test. NR3B$^{-/-}$ and $^{+/+}$ mice were tested on an accelerating rotarod. The $^{-/-}$ animals showed a significantly impaired performance compared with the $^{+/+}$ animals. The statistical significance tested by two-way repeated-measures ANOVA is indicated in the Figure. The performance significantly improved over time in $^{+/+}$ mice (trial effect, $P < 0.0001$ during the first six trials) but did not significantly change in $^{-/-}$ animals (trial effect, $P = 0.0756$); $n = 18$ for $^{-/-}$ and 15 for $^{+/+}$ animals.

intake). When the amount of water intake was corrected for the reduction of weight, the reduction of water intake was mostly cancelled out (not shown).

Abnormal motor function and increased social interaction of NR3B$^{-/-}$ mice

We then subjected the mice to a battery of behavioral tests (Table 1). Given the strong expression of NR3B in the motoneurons, the most informative tests would be the ones detecting somatomotor abilities. The result of the accelerating rotarod test was consistent with mildly impaired motor coordination or learning in $^{-/-}$ animals (genotype effect, $P = 0.0039$; Fig. 5). In the NR3B$^{+/+}$ animals, the performance was improved after a few trials (one-way repeated-measures ANOVA of the first six trials: trial effect, $F_{14,5} = 9.719$, $P < 0.0001$); however, in $^{-/-}$ animals, the performance remained almost at the same level throughout the session (trial effect: $F_{17,5} = 2.081$, $P = 0.0756$). We performed this test when the mice were 11–13 weeks old, when the difference in body weight was not significant (Fig. 4A). Generally, lighter animals perform better in rotarod tests, yet the NR3B$^{-/-}$ animals still performed below par despite their advantage. Therefore, the difference in performance could not be explained by the difference in body weight. In the beam test, $^{-/-}$ animals showed a slight but significant reduction in the total distance they walked compared with $^{+/+}$ animals, but other measures were not significantly impaired (supplementary Fig. S1, B–G). Overall, these test results were consistent with a mild motor impairment in NR3B$^{-/-}$ animals.

We then monitored the basal activity levels of the mice in their familiar environment. NR3B$^{-/-}$ animals showed a decreased activity in the home-cage behavioral test (Fig. 6A and B; two-way repeated-measures ANOVA, genotype effect, $F_{1,14} = 10.794$, $P = 0.0054$). Both NR3B$^{-/-}$ and $^{+/+}$ mice had a characteristic circadian rhythm and had a higher activity level during the dark phase of the cycle (Fig. 6A). Upon comparison of the two genotypes, we found that NR3B$^{-/-}$ animals were in general hypoactive, showing $\sim$30 and 50% less activity than $^{+/+}$ animals during dark and light cycles, respectively (Fig. 6A and B).

Interestingly, social interaction with a familiar cagemate in the home cage was significantly increased in NR3B$^{-/-}$ animals (Fig. 6C and D; two-way repeated-measures ANOVA, genotype effect, $F_{1,14} = 32.141$, $P < 0.0001$). To test whether this change in social interaction was a secondary effect due to the reduced activity in NR3B$^{-/-}$ animals, we plotted the social interaction vs. activity level for each time point so that we could compare the social interaction while animals were at similar activity levels (Fig. 6E and F). Overall two-way repeated-measures ANOVA showed significant genotype × activity level interaction in the dark phase ($F_{80,1120} = 6.965$, $P < 0.0001$) and in the light phase ($F_{40,560} = 2.196$, $P < 0.0001$). Social interaction in NR3B$^{-/-}$ animals was significantly higher, especially when the animals of both genotypes were at low activity levels in the dark phase (two-way repeated-measures ANOVA for activity levels from 0 to 200: genotype effect, $F_{1,14} = 18.538$, $P = 0.0007$) and in the light phase (two-way repeated-measures ANOVA for activity levels from 0 to 200: genotype effect,

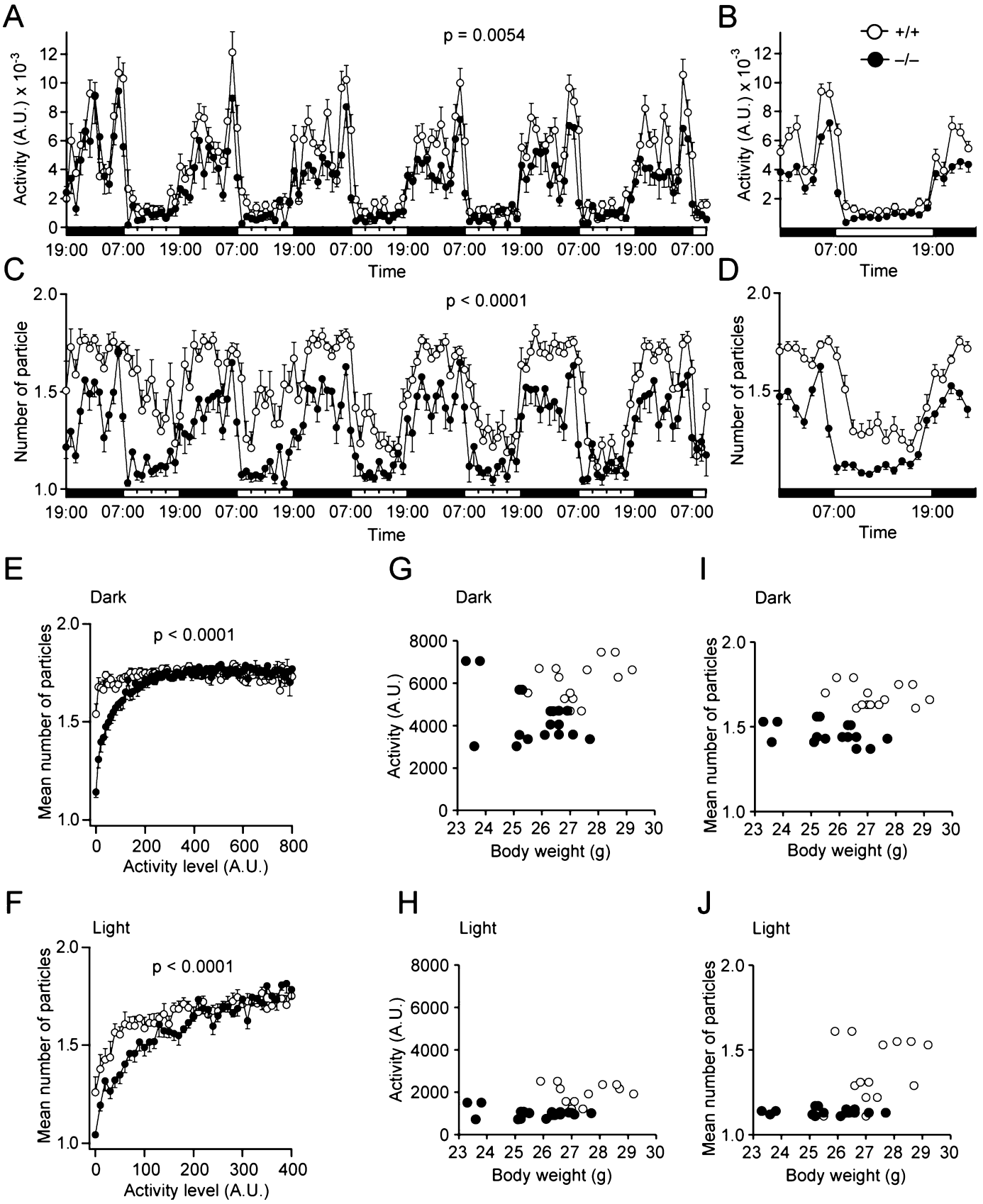

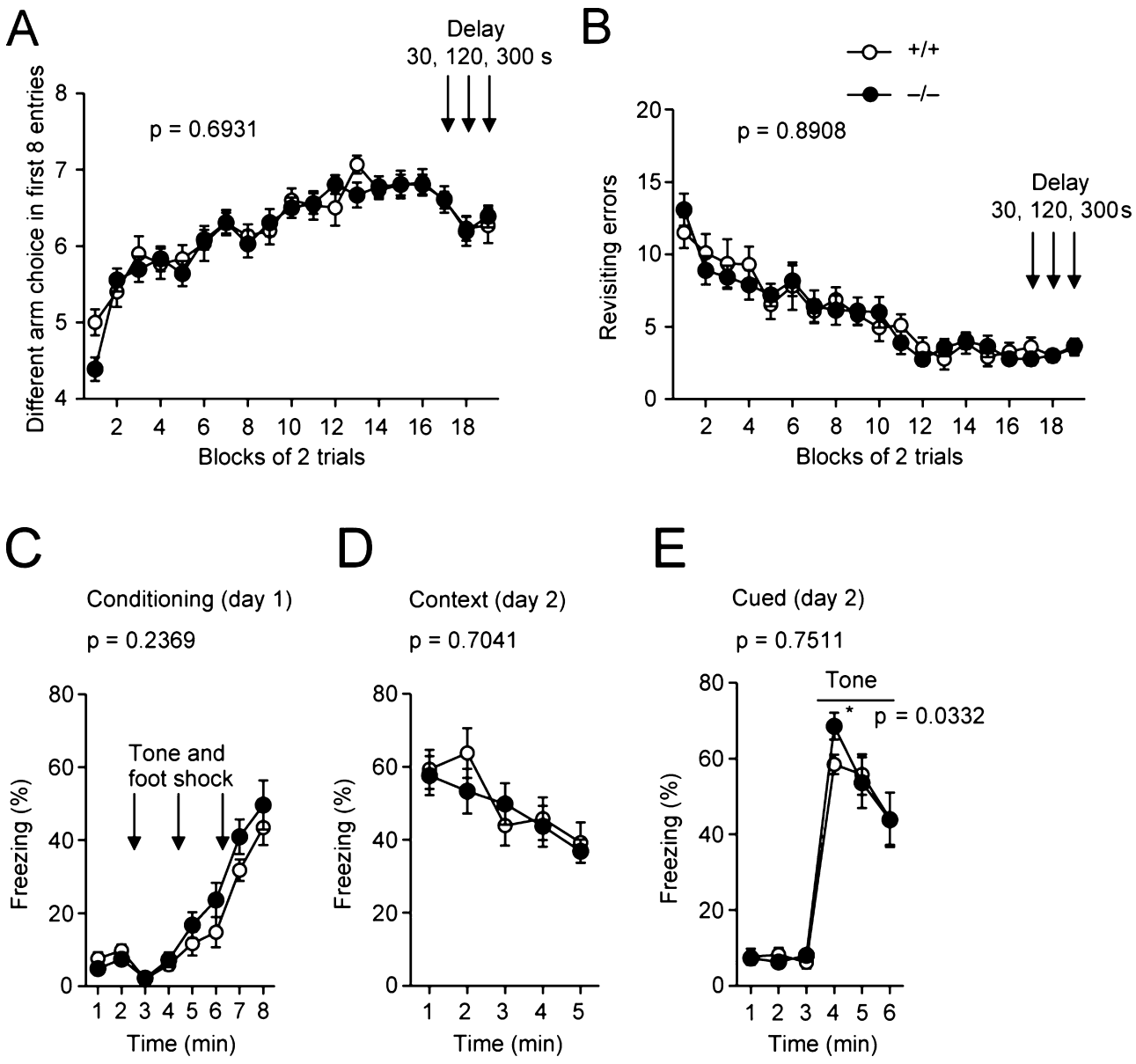

FIG. 7. Intact learning and memory in NR3B$^{-/-}$ animals. Learning ability of NR3B$^{-/-}$ animals was tested using an eight-arm radial maze and fear conditioning tests. (A and B) Performance of NR3B$^{-/-}$ and $^{+/+}$ mice in the eight-arm radial maze. (A) Number of different arms chosen within the first eight choices and (B) number of revisiting errors are shown. (C–E) Performance on fear conditioning test. (C) Freezing during conditioning phase, (D) contextual testing conducted 1 day after conditioning and (E) cued test with altered context are shown. There were no significant differences between genotypes in either the radial maze test or the fear conditioning except for the first time point after the tone in the cued test;. $n = 18$ for $^{-/-}$ and 15 for $^{+/+}$ animals. Tested with two-way repeated-measures ANOVA.

$F_{1,14} = 6.476$, $P = 0.0234$), while there were no significant genotype effects at higher activity levels (dark phase: two-way repeated-measures ANOVA for activity levels from 201 to 800: genotype effect, $F_{1,14} = 0.127$, $P = 0.7272$; light phase: two-way repeated-measures ANOVA for activity levels from 201 to 400: genotype effect, $F_{1,14} = 0.052$, $P = 0.8236$). Therefore, the increased social interaction between a pair of NR3B$^{-/-}$ animals in the same home cage was not simply a reflection of their generally reduced activity level.

FIG. 6. Altered home cage activity in NR3B$^{-/-}$ animals. Two animals of the same genotype were put in a home cage and their activity was monitored over an ~5.5-day period. (A) Decreased home cage activity of NR3B$^{-/-}$ animals. Activity levels are expressed in arbitrary units (A.U.) integrated for each hour and significance tested with one-way ANOVA. (B) Average of activity during days 1.5–5.5. (C) Increased social interaction with familiar cagemate in NR3B$^{-/-}$ animals. The social interaction is expressed as the number of particles in the image of the cage found by automatic detection. When the animals are separated, the particle number is two. When they are together, the number is one. Each dot indicates average per hour. Statistical significance was tested with one-way ANOVA. (D) Average social interaction during days 1.5–5.5. (E and F) Plot of activity level vs. social interaction. Activity level (A.U. in 2 min) was binned at a width of 10 and the averaged number of particles were obtained for each cage, averaged, and plotted for (E) the dark phase and (F) the light phase. Data for activity levels (E) > 800 or (F) > 400 are not shown, as they contain only small a number of entries (< 5% of total points) and the data points were scattered. Tested by two-way repeated measures ANOVA; $n = 9$ for $^{-/-}$ and 7 for $^{+/+}$ animals. (G and H) Plots of body weight vs. home cage activity in (G) dark and (H) light phases. (I and J) Plot of weight vs. social interaction in (I) dark and (J) light phases; $n = 18$ for $^{-/-}$ and 14 for $^{+/+}$ animals.

As we previously found that there is a significant positive correlation between body weight and home cage behaviour (T. Miyakawa, unpublished observation), we also compared activity levels or social interactions with body weight (Fig. 6G–J). The results show a difference in activity level and social interaction even within a range where the body weights of the two genotypes were similar to each other. This ruled out the possibility that the increased social interaction in mutants was merely the consequence of reduced body weight.

In grip-strength and wire-hang tests, the performances were similar in $^{-/-}$ and $^{+/+}$ animals, indicating that general muscular functions were not impaired (supplementary Fig. S1, H and I).

NMDAR-mediated learning was normal in NR3B$^{-/-}$ animals

NMDARs have been implicated in learning and memory. A low level of expression of NR3B was observed in the hippocampus, a

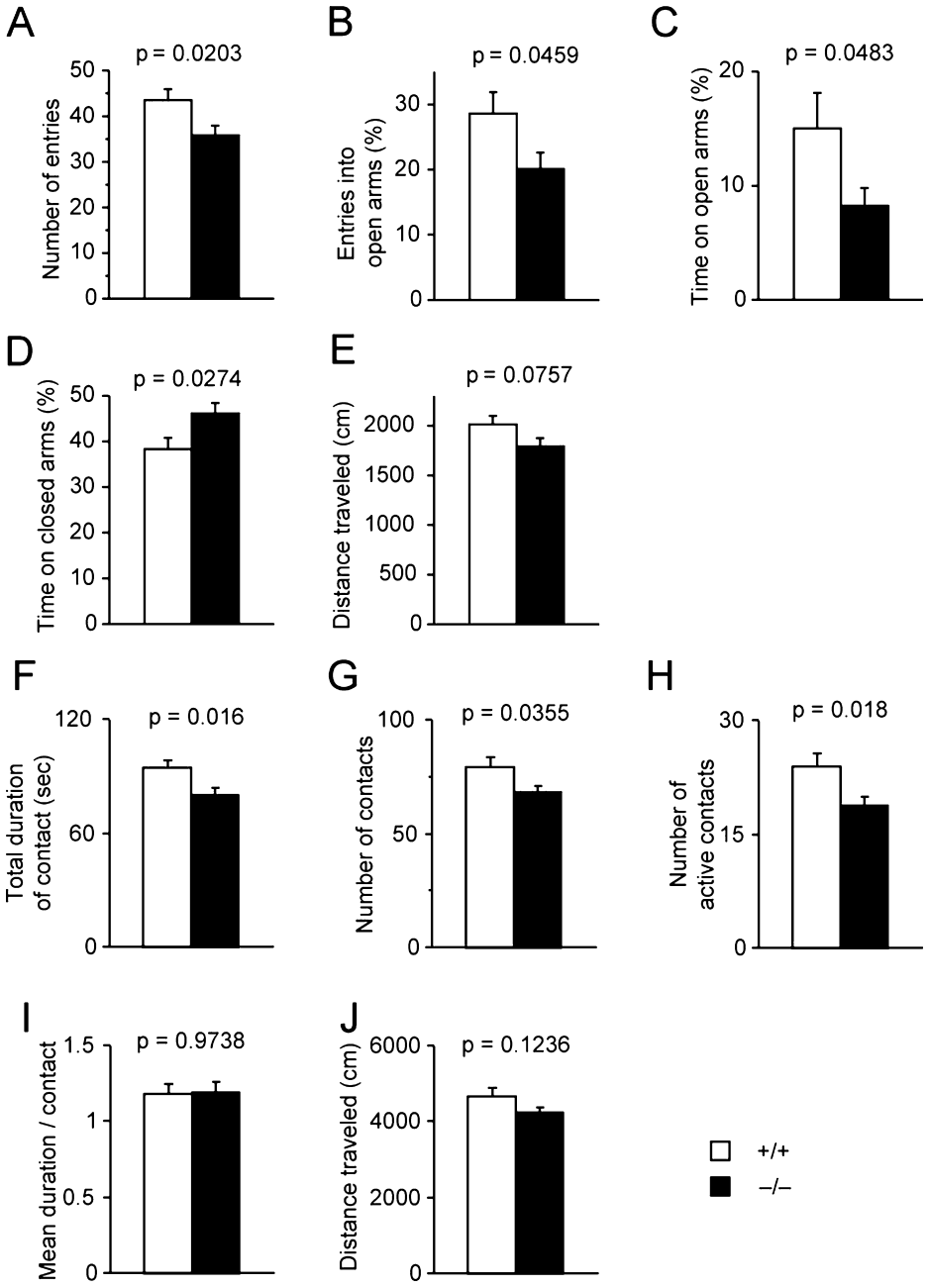

FIG. 8. Altered emotional levels in NR3B$^{-/-}$ animals. NR3B$^{-/-}$ mice were subjected to the elevated plus-maze and the social interaction tests. (A–E) The results of the elevated plus-maze test. (A) Total number of arm entries (both open and closed arms), (B) percentage entries into open arms out of total number of entries, (C) percentage of time spent in open arms, (D) percentage of time spent in closed arm and (E) distance traveled; $n = 18$ for $^{-/-}$ and 15 for $^{+/+}$ animals. (F–J) Social interaction with an unfamiliar mouse of the same genotype. (F) Total duration of contact, (G) number of contacts, (H) number of active contacts, (I) mean duration per contact, and (J) distance traveled; $n = 9$ for $^{-/-}$ and 7 for $^{+/+}$ animals. Tested with one-way ANOVA. These results are consistent with increased anxiety level in NR3B$^{-/-}$ animals.

critical brain structure involved in learning and memory (Matsuda *et al*., 2002; Bendel *et al*., 2005; GENSAT database). Therefore, it was intriguing to test whether there was any impairment of learning in NR3B$^{-/-}$ animals. We tested these animals with a radial maze test, a task dependent on both working and reference memories and requiring hippocampal function (Fig. 7A and B; Crawley, 1999). We did not see any difference in learning between NR3B$^{-/-}$ and $^{+/+}$ animals. We also tested contextual and cued fear conditioning tests which are, respectively, largely dependent on the hippocampus and amygdala (Fig. 7C–E; Crawley, 1999). These tests also did not show any difference in response between NR3B$^{-/-}$ and $^{+/+}$ animals except for the first time point after the tone in the cued test, which showed a small ($\sim$ 17%) increase. These results indicate that the contribution of NR3B to learning of these paradigms was largely insignificant.

Altered emotional status in NR3B$^{-/-}$ animals

We performed multiple additional tests included in the behavioral test battery. As a result, we found a behavioral phenotype indicating that the NR3B$^{-/-}$ mice had an altered emotional status. In the elevated plus-maze test (Fig. 8A–E), the NR3B$^{-/-}$ animals entered the arms significantly less frequently (genotype effect, $F_{1,31} = 5.981$, $P = 0.0203$), especially the open arms (genotype effect, $F_{1,31} = 4.327$, $P = 0.0459$), and spent significantly less time there (genotype effect, $F_{1,31} = 4.227$, $P = 0.0483$; Fig. 8A–C). These were not merely a reflection of reduced general activity because the time the animals spent in the closed arms was significantly higher (genotype effect, $F_{1,31} = 5.359$, $P = 0.0274$; Fig. 8D) and the numbers of entries into the closed arms were similar (data not shown). Also, the total distances traveled were not significantly different (genotype effect, $F_{1,31} = 3.378$, $P = 0.0757$; Fig. 8E).

In the social interaction test in the novel environment (Fig. 8F–J), when the animals were exposed to unfamiliar animals, the interaction was significantly less (total duration of contact, $F_{1,14} = 7.493$, $P = 0.0160$; number of contacts, $F_{1,14} = 5.416$, $P = 0.0355$; Fig. 8F and G.) The total distance traveled was not significantly different (genotype effect, $F_{1,14} = 2.685$, $P = 0.1236$; Fig. 8J), ruling out the possibility that the reduction in the interaction was merely a reflection of a decreased general activity level. These results are consistent with an increased anxiety level. To further explore the emotional status, we applied the open-field test paradigm (Fig. 9A–E). NR3B$^{-/-}$ animals showed a statistically significant reduction in stereotypic activity, especially when the animals were first introduced into the new environment (genotype $\times$ time interaction, $F_{23,713} = 1.545$, $P = 0.048$; genotype effect in first 1 min, $F_{1,31} = 10.302$, $P = 0.0031$; Fig. 9D and E) but they were otherwise similar to $^{+/+}$ animals. We also performed a light–dark transition (supplementary Fig. S3) test and Porsolt forced-swim test, neither of which showed any difference between NR3B$^{-/-}$ and $^{+/+}$ animals.

In view of the results suggesting an altered emotional level in NR3B$^{-/-}$ animals, we examined the cytoarchitecture of the amygdaloid body using Cresyl violet Nissl staining (Fig. 10). We

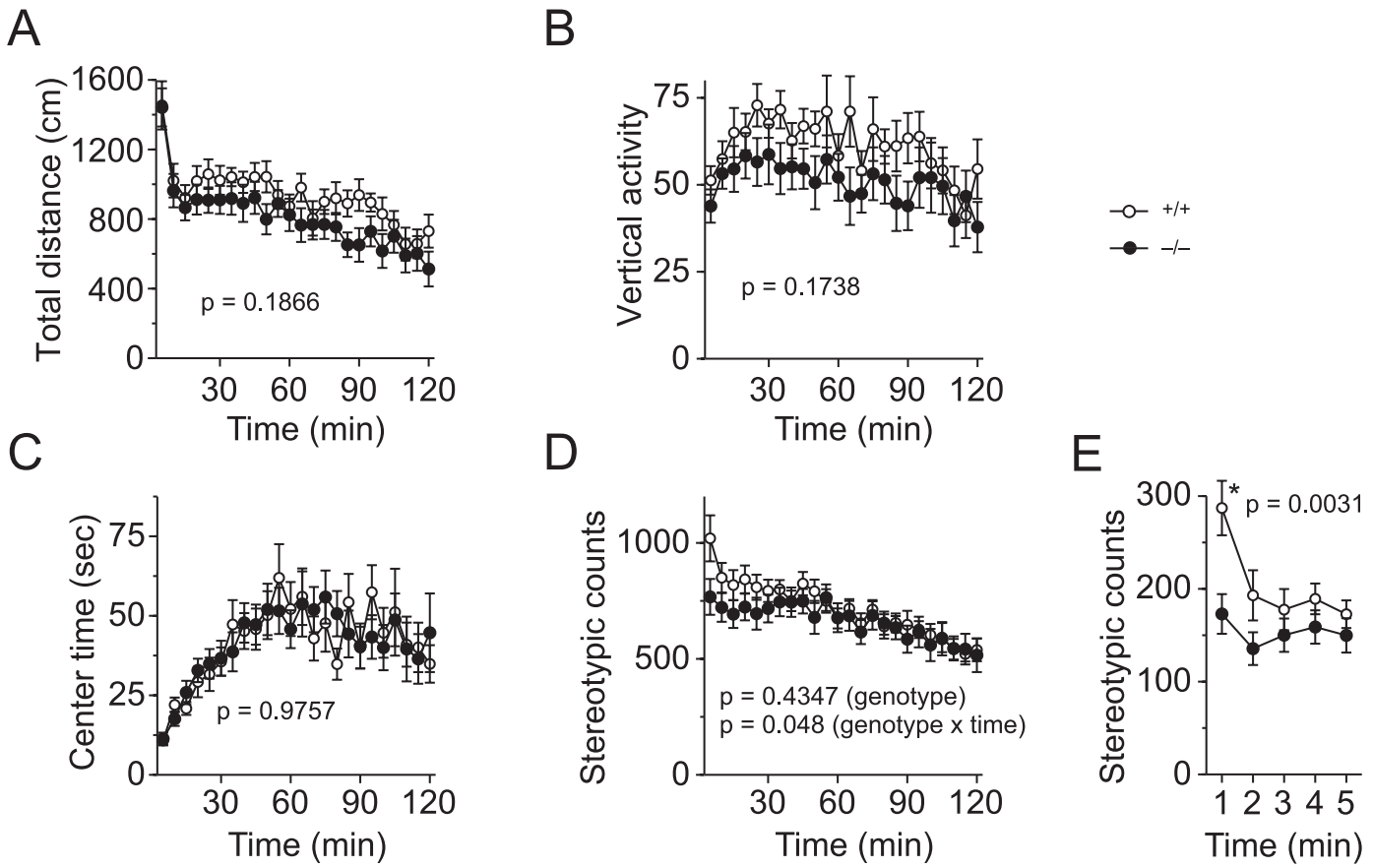

FIG. 9. A mild change in the open-field test in NR3B$^{-/-}$ mice. The NR3B$^{-/-}$ animals were subject to open-field tests. (A) Total locomotion distance. (B) Count of vertical activity. (C) Time spent on the centre of the field. (D) Count of stereotypic behaviour. (E) Breakdown of the first 5 min of stereotypic counts, in 1-min intervals; $n = 18$ for $^{-/-}$ and 15 for $^{+/+}$ animals. Tested with two-way repeated-measures ANOVA.

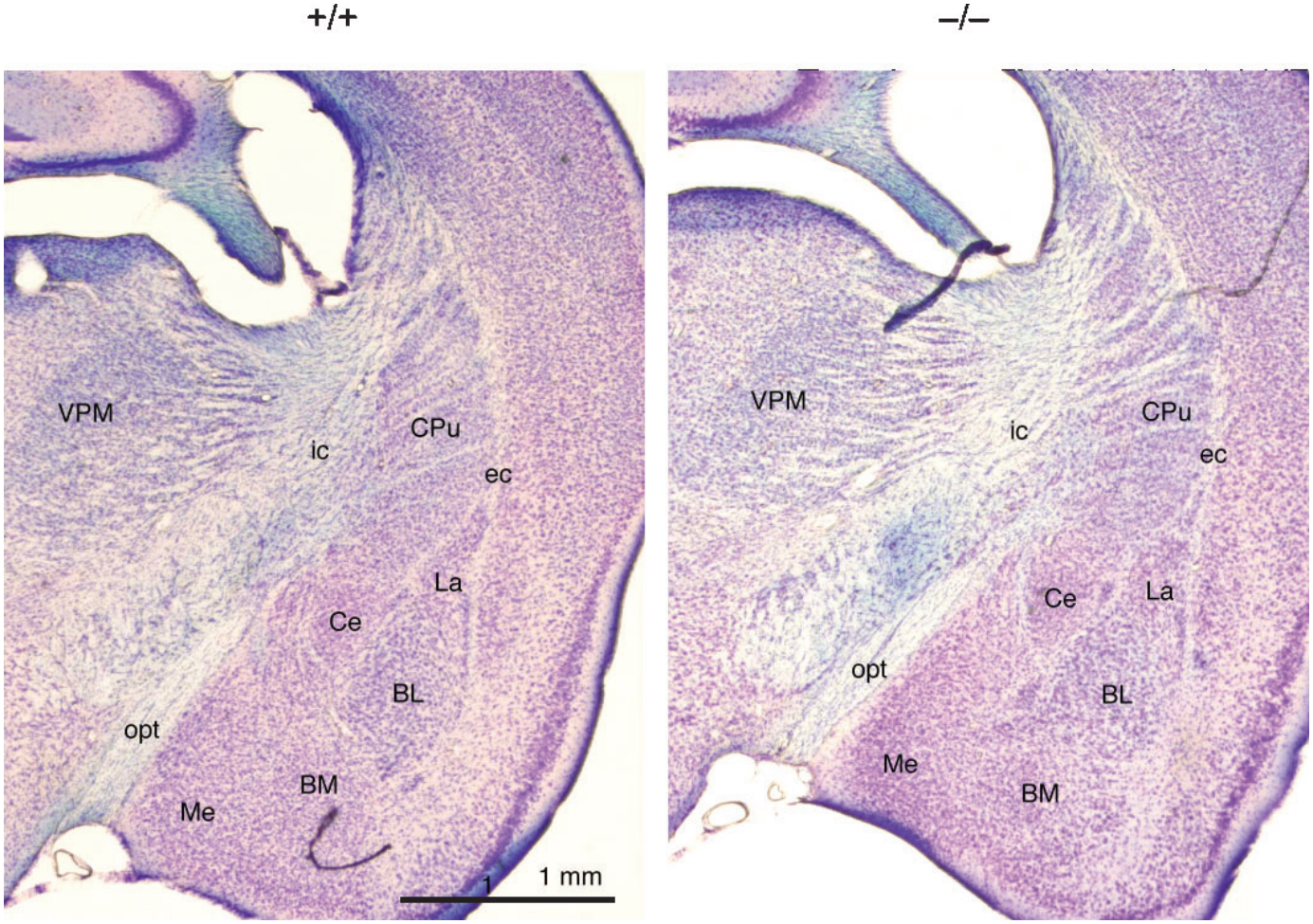

FIG. 10. Cytoarchitecture of the amygdala was normal in NR3B$^{-/-}$ mice. Coronal sections of brain from NR3B$^{-/-}$ and littermate control (7 months old) containing amygdala are shown. The sections were stained with Nissl staining. BL, basolateral amygdaloid nucleus; BM, basomedial amygdaloid nucleus; La, lateral amygdaloid nucleus; CPu, caudate–putamen; ec, external capsule; ic, internal capsule; Me, medial amygdaloid nucleus; opt, optic tract; VPM, ventral posterolateral thalamic nucleus.

did not detect any apparent difference between NR3B$^{+/+}$ and $^{-/-}$ animals.

Discussion

NR3B$^{-/-}$ animals showed mild impairment in motor functions

To study the effect of loss of NR3B on behaviour and neuromuscular function, we generated a mouse model by genetically ablating the NR3B gene. Our NR3B$^{-/-}$ animals were overall healthy, consistent with our recent observation of homozygous occurrence of a NR3B null mutation in the absence of a clinical phenotype in human. Upon further investigation, the NR3B$^{-/-}$ mice had a mild but significant motor phenotype, evident from impaired performance in the rotarod test, consistent with strong expression of NR3B in WT spinal motoneurons. As motoneuron viability and muscular strength appear normal in these mice, the most likely explanation is that this was due to an altered excitatory synaptic transmission in motoneurons. However, we cannot totally rule out the possibility that it was due to dysfunction of other nervous system components in which low-level expression of NR3B was detected. NR3B is expressed in the structures involved in motor learning and coordination, including the cerebellum and vestibular nuclei (Nishi *et al*., 2001; Chatterton *et al*., 2002; Matsuda *et al*., 2002; GENSAT database). Therefore, it is still possible that the loss of NR3B from these regions, either alone or combined with expression in spinal cord, contributed to the observed motor impairment. The reduced activity level in the home cage compared to that of littermate controls may also be the result of altered transmission in motoneurons as well.

The loss of NR3B can have two different consequences depending on the presence or absence of the NR2 subunit in the receptor complex. In neurons where NR2 is expressed, NR3B associates with both NR1 and NR2 to inhibit the receptor activity (Nishi *et al*., 2001; Matsuda *et al*., 2002). Then the loss of NR3B will lead to an increase in NMDAR current. In neurons lacking NR2, NR3B associates only with NR1, and composes glycinergic receptors (Chatterton *et al*., 2002). In such neurons, the loss of NR3B will lead to a loss of excitatory glycinergic input. In motoneurons, NR1 is expressed continually throughout life while NR2 expression gradually decreases during early postnatal life and NR3B gradually increases (Oshima *et al*., 2002; Fukaya *et al*., 2005). We attempted to compare synaptic and ligand-induced current in acute preparations from both WT and NR3B$^{-/-}$ mice to prove or disprove the presence of a proposed excitatory glycinergic current in motoneurons, but the techniques of recording from postnatal motoneurons (> P14) have not been well established and, due to the difficulties of such

experiments, we have been unable to obtain reliable recordings from them. Therefore, how NMDAR-mediated synaptic transmission in motoneurons is involved in motor coordination and learning, and how it is actually altered by the loss of NR3B, are still open questions.

Our mice differ from NR3B-knockout animals examined by another group (Qu *et al*., 2004), which show a progressive paresis of extremities by P3 and early postnatal death by P5. Their observations also do not reconcile with our observations of the ontogenetic expression profile of NR3B in motoneurons, which appears after P10 (Fukaya *et al*., 2005). The reason for this discrepancy is not clear at this point. The conclusion awaits further characterization of their knockout animals as the results are published only in abstract form (Qu *et al*., 2004).

NR3B$^{-/-}$ animals had a nonmotoneuronal phenotype

The NR3B$^{-/-}$ animals also showed phenotypes not readily accountable by the motoneuronal expression. In the elevated maze test, the time spent in the open arm and the entry into open arms were significantly reduced. In the social interaction test with an unfamiliar mouse, the interaction was also reduced. In contrast, in the home cage the social interaction of NR3B$^{-/-}$ mice with familiar cagemates was increased compared to $^{+/+}$ animals. These observations can be considered a result of change in emotional level of the animals. A low level of expression of NR3B is detected in amygdala (GENSAT database), a primary brain region implicated in emotional behaviour and, therefore, the loss of NR3B may change the synaptic functions or fine structure below the resolution of the experiments in this study, resulting in these changes in the NR3B$^{-/-}$ animals. From this perspective, the observed motor impairment and reduction in the activity level in the home cage may also arise from a change in the emotional status, not directly from the impairment in motoneuronal synaptic transmission; NR3B$^{-/-}$ may more quickly become weary of walking on the rotarod or platform because their emotional status is significantly affected. A future study using a region-specific knockout will be useful for distinguishing these possibilities.

The neuronal mechanism of emotion is closely linked to NMDAR activity (Javitt, 2004). An exposure to stress produces a robust increase in glutamate release and increases NMDAR expression in regions mediating emotional behaviour (Moghaddam, 1993; Bartanusz *et al*., 1995; Singewald *et al*., 1995; Fitzgerald *et al*., 1996). Pharmacological or genetic manipulation of NMDAR function or downstream signalling also results in changes in emotion-related behaviors (Wiley *et al*., 1995; Mohn *et al*., 1999; Miyakawa *et al*., 2003; Boyce-Rustay & Holmes, 2006). Interestingly, these manipulations decreasing NMDAR function in animals resulted in anxiolytic changes, such as increased time spent in the open arm in the elevated plus-maze and decreased social interaction in the home cage, which is opposite to the changes seen in NR3B$^{-/-}$ animals. The phenotype of NR3B$^{-/-}$ animals is, in fact, consistent with the inhibitory role of NR3B; the loss of inhibitory NR3B disinhibits the NMDAR and increases the overall activity as opposed to previous pharmacological and genetic studies.

We did not see a large effect of the loss of NR3B in open-field and light–dark transition tests, both of which have also been used to test anxiety levels. We have recently conducted a factor analysis of a large set of data obtained from >2900 mice, including the WT and the mutants from 53 genetically engineered strains, which were tested in the laboratory of T.M. using the same behavioral test battery (Yamasaki *et al*., 2006). This analysis indicates that the parameters obtained from these tests do not necessarily correlate with each other even though the tests are all designed to detect the anxiety level or at least treat the anxiety level as a major component. A plausible explanation is that these tests are sensitive to the different aspects of the anxiety mechanisms and are not necessarily affected to the same extent by a given manipulation.

The NR3B$^{-/-}$ had lighter body weight, although food and water intake appeared the same (Fig. 4) and histological analysis also did not show any change suggestive of metabolic impairment (not shown). The muscular strength (supplementary Fig. S1) and innervation appeared normal (Fig. 3), ruling out muscular atrophy due to denervation. Increased anxiety levels may cause reduced body weight but otherwise we currently do not have any explanation for this reduction in body weight.

In view of these phenotypes observed in NR3B$^{-/-}$ mice, it would be intriguing to examine human individuals with and without NR3B using tests designed to assess various emotional attributes. The lack of NR3B appears not to negatively affect the survival of homozygous carrier individuals, as these carriers are prevailing worldwide. However, there is a certain variance in the distribution of allele frequencies in different human populations. Thus it will also be intriguing to see the relation of allele frequency in different geographical populations and their cultural propensity.

Supplementary material

The following supplementary material may be found on
http://www.blackwell-synergy.com

Appendix. S1. Supplementary methods, including:
Fig. S1. Basic physical test and motor test in NR3B$^{-/-}$ mouse.
Fig. S2. Sensory and motor reflex tests in NR3B$^{-/-}$ mouse.
Fig. S3. Light/dark transition test and Porsolt forced swim test in NR3B$^{-/-}$ mouse.

Please note: Blackwell Publishing is not responsible for the content or functionality of any supplementary materials supplied by the authors. Any queries (other than missing material) should be directed to the corresponding author for the article.

Acknowledgements

We thank Drs Brigitte van Zundert, Mark C. Bellingham, Martha Constantin-Paton, Robert G. Kalb, Makoto Urushitani and Ryosuke Takahashi for carrying out various preliminary analyses of the mouse strain described here, and Dr Thomas McHugh for comments on the manuscript. Y.H. was supported by RIKEN, the Ellison Medical Foundation, NIH grants R21NS46421 and R01DA17310, M.F. by Grants-in-Aid for Scientific Research on Priority Areas (18053001) from the Ministry of Education, Culture, Sports, Science and Technology of Japan, M.W. by Grants-in-Aid for Exploratory research (17650087) from the Ministry of Education, Culture, Sports, Science and Technology of Japan, T.M. by a Grant-in-Aid from the Institute for Bioinformatics Research and Development (BIRD) of Japan Science and Technology Agency and a Grant-in-Aid for Young Scientists (A; 16680015) from the Ministry of Education, Culture, Sports, Science and Technology of Japan, and R.H.B. by NIH grants 1P01NS31248-02 and R01NS37912, Project ALS, the ALS Association, the Pierre L. de Bourgknecht ALS Research Foundation, the Al-Athel Foundation, the ALS Therapy Alliance and the Angel Fund for ALS Research, and the Muscular Dystrophy Association.

Abbreviations

ES, embryonic stem; MUNE, motor unit number estimation; NMDAR, *N*-methyl-D-aspartate receptor; P, postnatal day; VAchT, vesicular acetylcholine transporter; WT, wild-type.

References

Andersson, O., Stenqvist, A., Attersand, A. & von Euler, G. (2001) Nucleotide sequence, genomic organization, and chromosomal localization of genes encoding the human NMDA receptor subunits NR3A and NR3B. *Genomics*, **78**, 178–184.

Bartanusz, V., Aubry, J.M., Pagliusi, S., Jezova, D., Baffi, J. & Kiss, J.Z. (1995) Stress-induced changes in messenger RNA levels of N-methyl-D-aspartate and AMPA receptor subunits in selected regions of the rat hippocampus and hypothalamus. *Neuroscience*, **66**, 247–252.

Bendel, O., Prunell, G., Stenqvist, A., Mathiesen, T., Holmin, S., Svendgaard, N.A. & von Euler, G. (2005) Experimental subarachnoid hemorrhage induces changes in the levels of hippocampal NMDA receptor subunit mRNA. *Brain Res. Mol. Brain Res.*, **137**, 119–125.

Boyce-Rustay, J.M. & Holmes, A. (2006) Genetic inactivation of the NMDA receptor NR2A subunit has anxiolytic- and antidepressant-like effects in mice. *Neuropsychopharmacology*, **31**, 2405–2414.

Chatterton, J.E., Awobuluyi, M., Premkumar, L.S., Takahashi, H., Talantova, M., Shin, Y., Cui, J., Tu, S., Sevarino, K.A., Nakanishi, N., Tong, G., Lipton, S.A. & Zhang, D. (2002) Excitatory glycine receptors containing the NR3 family of NMDA receptor subunits. *Nature*, **415**, 793–798.

Ciabarra, A.M., Sullivan, J.M., Gahn, L.G., Pecht, G., Heinemann, S. & Sevarino, K.A. (1995) Cloning and characterization of χ-1: a developmentally regulated member of a novel class of the ionotropic glutamate receptor family. *J. Neurosci.*, **15**, 6498–6508.

Crawley, J.N. (1999) *What's Wrong with My Mouse? Behavioral Phenotyping of Transgenic and Knockout Mice*. Wiley-Liss, New York.

Fitzgerald, L.W., Ortiz, J., Hamedani, A.G. & Nestler, E.J. (1996) Drugs of abuse and stress increase the expression of GluR1 and NMDAR1 glutamate receptor subunits in the rat ventral tegmental area: common adaptations among cross-sensitizing agents. *J. Neurosci.*, **16**, 274–282.

Fukaya, M., Hayashi, Y. & Watanabe, M. (2005) NR2 to NR3B subunit switchover of NMDA receptors in early postnatal motoneurons. *Eur. J. Neurosci.*, **21**, 1432–1436.

Garcia, M.L., Lobsiger, C.S., Shah, S.B., Deerinck, T.J., Crum, J., Young, D., Ward, C.M., Crawford, T.O., Gotow, T., Uchiyama, Y., Ellisman, M.H., Calcutt, N.A. & Cleveland, D.W. (2003) NF-M is an essential target for the myelin-directed 'outside-in' signaling cascade that mediates radial axonal growth. *J. Cell Biol.*, **163**, 1011–1020.

Gomi, H., Yokoyama, T., Fujimoto, K., Ikeda, T., Katoh, A., Itoh, T. & Itohara, S. (1995) Mice devoid of the glial fibrillary acidic protein develop normally and are susceptible to scrapie prions. *Neuron*, **14**, 29–41.

Gong, S., Zheng, C., Doughty, M.L., Losos, K., Didkovsky, N., Schambra, U.B., Nowak, N.J., Joyner, A., Leblanc, G., Hatten, M.E. & Heintz, N. (2003) A gene expression atlas of the central nervous system based on bacterial artificial chromosomes. *Nature*, **425**, 917–925.

Javitt, D.C. (2004) Glutamate as a therapeutic target in psychiatric disorders. *Mol. Psychiatry*, **9**, 984–997.

Magdaleno, S., Jensen, P., Brumwell, C.L., Seal, A., Lehman, K., Asbury, A., Cheung, T., Cornelius, T., Batten, D.M., Eden, C., Norland, S.M., Rice, D.S., Dosooye, N., Shakya, S., Mehta, P. & Curran, T. (2006) BGEM: an in situ hybridization database of gene expression in the embryonic and adult mouse nervous system. *PLoS Biol.*, **4**, e86.

Matsuda, K., Fletcher, M., Kamiya, Y. & Yuzaki, M. (2003) Specific assembly with the NMDA receptor 3B subunit controls surface expression and calcium permeability of NMDA receptors. *J. Neurosci.*, **23**, 10064–10073.

Matsuda, K., Kamiya, Y., Matsuda, S. & Yuzaki, M. (2002) Cloning and characterization of a novel NMDA receptor subunit NR3B: a dominant subunit that reduces calcium permeability. *Brain Res. Mol. Brain Res.*, **100**, 43–52.

Miyakawa, T., Leiter, L.M., Gerber, D.J., Gainetdinov, R.R., Sotnikova, T.D., Zeng, H., Caron, M.G. & Tonegawa, S. (2003) Conditional calcineurin knockout mice exhibit multiple abnormal behaviors related to schizophrenia. *Proc. Natl. Acad. Sci. USA*, **100**, 8987–8992.

Miyakawa, T., Yamada, M., Duttaroy, A. & Wess, J. (2001) Hyperactivity and intact hippocampus-dependent learning in mice lacking the M1 muscarinic acetylcholine receptor. *J. Neurosci.*, **21**, 5239–5250.

Moghaddam, B. (1993) Stress preferentially increases extraneuronal levels of excitatory amino acids in the prefrontal cortex: comparison to hippocampus and basal ganglia. *J. Neurochem.*, **60**, 1650–1657.

Mohn, A.R., Gainetdinov, R.R., Caron, M.G. & Koller, B.H. (1999) Mice with reduced NMDA receptor expression display behaviors related to schizophrenia. *Cell*, **98**, 427–436.

Nakanishi, S. & Masu, M. (1994) Molecular diversity and functions of glutamate receptors. *Annu. Rev. Biophys. Biomol. Struct.*, **23**, 319–348.

Niemann, S., Landers, J.E., Churchill, M.J., Hosler, B., Sapp, P., Speed, W.C., Lahn, B.T., Kidd, K.K., Brown,R.H. Jr & Hayashi, Y. (in press) Motoneuron-specific NR3B gene: No association with ALS and evidence for a common null allele. *Neurology*, in press [epub ahead of print doi:10.1212/01.wnl.0000271078.51280.17].

Nishi, M., Hinds, H., Lu, H.P., Kawata, M. & Hayashi, Y. (2001) Motoneuron-specific expression of NR3B, a novel NMDA-type glutamate receptor subunit that works in a dominant-negative manner. *J. Neurosci.*, **21**, RC185.

Oshima, S., Fukaya, M., Masabumi, N., Shirakawa, T., Oguchi, H. & Watanabe, M. (2002) Early onset of NMDA receptor GluR ε1 (NR2A) expression and its abundant postsynaptic localization in developing motoneurons of the mouse hypoglossal nucleus. *Neurosci. Res.*, **43**, 239–250.

Qu, M., Chatterton, J.E., Wang, R., Huang, L., Millan, J., Lipton, S.A. & Zhang, D. (2004) Severe motor neuron loss in the spinal cord of NMDA receptor subunit 3B (NR3B) null mice in the early postnatal period. *Soc. Neurosci. Abstr.*, 957.3.

Rudnicki, M.A., Braun, T., Hinuma, S. & Jaenisch, R. (1992) Inactivation of MyoD in mice leads to up-regulation of the myogenic HLH gene Myf-5 and results in apparently normal muscle development. *Cell*, **71**, 383–390.

Sakai, K. & Miyazaki, J. (1997) A transgenic mouse line that retains Cre recombinase activity in mature oocytes irrespective of the cre transgene transmission. *Biochem. Biophys. Res. Commun.*, **237**, 318–324.

Seeburg, P.H. (1993) The TiPS/TINS lecture: the molecular biology of mammalian glutamate receptor channels. *Trends Pharmacol. Sci.*, **14**, 297–303.

Shefner, J.M., Cudkowicz, M. & Brown, R.H. Jr (2006) Motor unit number estimation predicts disease onset and survival in a transgenic mouse model of amyotrophic lateral sclerosis. *Muscle Nerve*, **34**, 603–607.

Singewald, N., Zhou, G.Y. & Schneider, C. (1995) Release of excitatory and inhibitory amino acids from the locus coeruleus of conscious rats by cardiovascular stimuli and various forms of acute stress. *Brain Res.*, **704**, 42–50.

Sucher, N.J., Akbarian, S., Chi, C.L., Leclerc, C.L., Awobuluyi, M., Deitcher, D.L., Wu, M.K., Yuan, J.P., Jones, E.G. & Lipton, S.A. (1995) Developmental and regional expression pattern of a novel NMDA receptor-like subunit (NMDAR-L) in the rodent brain. *J. Neurosci.*, **15**, 6509–6520.

Takao, K. & Miyakawa, T. (2006) Investigating gene-to-behavior pathways in psychiatric disorders: the use of a comprehensive behavioral test battery on genetically engineered mice. *Ann. NY Acad. Sci.*, **1086**, 144–159.

Watanabe, M., Fukaya, M., Sakimura, K., Manabe, T., Mishina, M. & Inoue, Y. (1998) Selective scarcity of NMDA receptor channel subunits in the stratum lucidum (mossy fibre-recipient layer) of the mouse hippocampal CA3 subfield. *Eur. J. Neurosci.*, **10**, 478–487.

Wiley, J.L., Cristello, A.F. & Balster, R.L. (1995) Effects of site-selective NMDA receptor antagonists in an elevated plus-maze model of anxiety in mice. *Eur. J. Pharmacol.*, **294**, 101–107.

Yagi, T., Nada, S., Watanabe, N., Tamemoto, H., Kohmura, N., Ikawa, Y. & Aizawa, S. (1993) A novel negative selection for homologous recombinants using diphtheria toxin A fragment gene. *Anal. Biochem.*, **214**, 77–86.

Yamasaki, N., Takao, K., Tanda, K., Toyama, K., Takahashi, Y., Yamagata, S. & Miyakawa, T. (2006) Factor analyses of large-scale data justify the behavioral test battery strategy to reveal the functional significances of the genes expressed in the brain. *Soc. Neurosci. Abstr.*, 100.15.